Investigating the Effects of Cure Pressure on Tool-Part Interaction and Process-induced Deformations in Composites

Caleb Schoenholz; Joann Moomaw; Navid Zobeiry

OFFICIAL CONFERENCE PUBLICATION

Proceedings of the American Society for Composites - Thirty-Seventh Technical Conference (2022)

https://doi.org/10.12783/asc37/36383

RELATED SUBSTANTIALLY EXTENDED JOURNAL ARTICLE

C. Schoenholz and N. Zobeiry, "Investigating the Impacts of Processing Variability on Tool-Part Interaction for Interply-Toughened Aerospace Composites Using a Novel Shear Technique," Composites Part A 178, 107973 (2024).

https://doi.org/10.1016/j.compositesa.2023.107973

ABSTRACT

The interaction between a tool and part during composites manufacturing may significantly contribute to the formation of residual stresses and process-induced deformations (PIDs). High levels of uncertainty are often associated with tool-part interaction and resulting PIDs due to the complex underlying physics, and variabilities and uncertaintieis in processing. During the assembly of aerospace composite structures, PIDs may create significant geometry mismatches and lead to a loss of mechanical performance. Aerospace manufacturers commonly use costly and time-consuming techniques such as shimming to compensate for PIDs and meet process specification requirements. Although process simulation tools have evolved significantly in recent years to enable mitigation of PIDs via tool geometry compensation, in practice, they are not implemented often due to challenges associated with the characterization and calibration of numerical models. One such challenge is accurately measuring the degree of tool-part interaction and interfacial stresses during processing cycles. This paper presents a custom-built test fixture to directly measure tool-part interfacial stress development during processing of composites. The experimental setup is installed in a Dynamic Mechanical Analyzer (DMA) for in-situ measurement of tool-part interfacial stresses. The technique allows for the evaluation of the effects of process parameters, including pressure, temperature, lay-up, and tool surface condition. In this study, tool-part stress development was characterized as a function of the applied pressure for Toray T800S/3900-2 laminates cured on steel tools treated with Frekote release agent. The characterized stresses were then validated by measuring warpages of long and symmetric laminates cured on flat steel tools using different pressures similar to DMA tests. Results demonstrated that cure pressure significantly impacts the multi-physics interactions between fibers, resin, interply tougheners, and the tool surface throughout a cure cycle. The results of this paper can be used to expand the current understanding of tool-part interaction and potentially mitigate PIDs in composites processing.

Caleb Schoenholz, Joann Moomaw, Navid Zobeiry*
Materials Science & Engineering Department, University of Washington, 302 Roberts Hall, Box 352120, Seattle, WA 98195-2120, U.S.A.
*Corresponding author, (206) 221-3254, navidz@uw.edu

INTRODUCTION

Aerospace composites manufacturing is a series of complex and interdependent processes that may lead to the formation of residual stresses in parts and, consequently, process-induced deformations (PIDs) [1-4]. Residual stresses develop during processing mainly due to a mismatch of free strains at the micro-, macro-, coupon-, and component-levels [1]. Other factors, however, may also significantly contribute to the formation of residual stresses and PIDs, including the interaction between a production tool and composite part [5-14]. This study investigates tool-part interaction between a flat unidirectional composite part with a $[90]_n$ lay-up and a steel production tool treated with a Frekote release coating. Fig. 1 shows a schematic of the underlying mechanisms and the resulting PIDs (i.e., warpage) involved in this scenario.

During autoclave processing, a large applied pressure pushes the tool and part together. At the same time, the system is subjected to a temperature cycle, resulting in the formation of tool-part interfacial physicochemical bonds. Production tools are typically prepared with release coatings prior to part lay-up to mitigate tool-part bonding. Although release coatings reduce interfacial bonding to some degree, they do not entirely mitigate tool-part interaction and PIDs [9]. For a $[90]_n$ laminate, elevated processing temperatures also cause mismatches in free strains between the tool and part due to thermal expansion differences and longitudinal cure shrinkage in the composite. When paired with interfacial bonds, these free strain mismatches create a shear interaction at the tool-part interface that transfers stresses into the tool-adjacent composite plies. Some of these stresses are alleviated during processing through interlaminar shear. However, a through-thickness stress gradient is developed and locked into the part as curing progresses. During the demolding process after a cure cycle, locked-in (i.e., residual) stresses are partially released through bending deformation, resulting in concave-up warpage of the initially flat laminate.

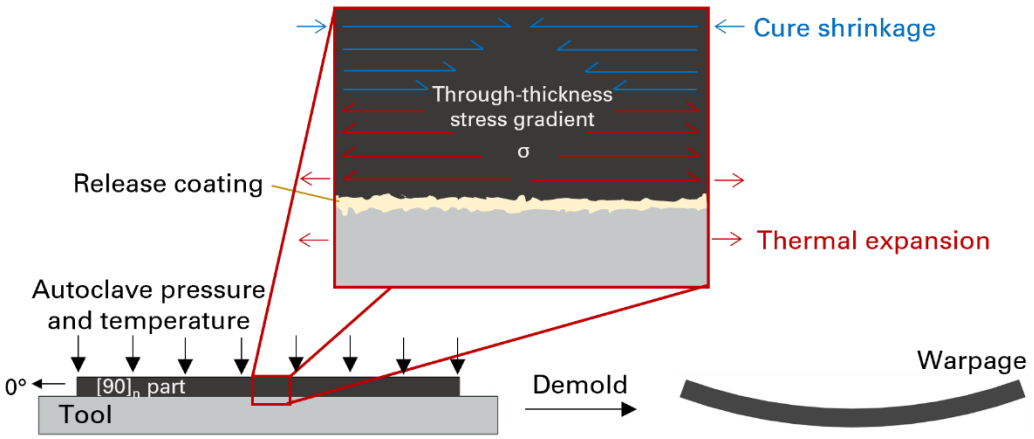

Figure 1. Schematic of tool-part interaction between a flat unidirectional composite part with a $[90]_n$ lay-up and a steel production tool during autoclave processing.

The magnitudes of tool-part interaction and PIDs in flat composite parts may be significantly influenced by both intrinsic parameters related to part geometry and material properties, and extrinsic parameters related to tooling and processing [12]. For example, a part's tool-side surface area, roughness, and material chemistry determine the magnitude of tool-part stresses generated [5,6]. Other intrinsic parameters such as thickness and lay-up affect a composite part's ability to alleviate residual stresses through interlaminar shear [9,13]. Extrinsic parameters such as the tool material (e.g., aluminum or Invar), surface condition (e.g., release agent or FEP), cure pressure, and temperature cycle are primarily responsible for the degree of physicochemical bonding and efficiency of tool-part interfacial stress transfer during processing [5,6,12,14].

Although there has been a considerable amount of work done in academia to understand the effects of process parameters on tool-part interaction and PIDs, many of these parameters remain surrounded by high levels of uncertainty. This is partly due to the challenge of accurately measuring the degree of tool-part interaction and interfacial stresses during processing cycles. Inherent material and process variabilities also serve as additional uncertainty sources. As a result, process simulation tools often rely on oversimplified and uncalibraited models to represent tool-part interaction. This may lead to errors in prediciting PIDs, causing mitigation techniques such as tool geometry compensation to be based on cost-deficient trial-and-error methods. Manufacturers are often forced to use assembly compensation methods such as shimming to counteract PIDs and meet process specification requirements. Unfortunately, in addition to cost considerations, such assembly compensation methods may introduce additional residual stresses in parts and consequently reduce mechanical performance.

This paper presents a custom-built technique to directly measure interfacial stresses and characterize tool-part interaction during processing cycles. The experimental setup is installed in a Dynamic Mechanical Analyzer (DMA) for quick in-situ measurement of tool-part interfacial stresses as a function of process parameters, including pressure, cure cycle, lay-up, and tool surface condition. In this study, the novel technique is used to investigate the effects of cure pressure on tool-part interfacial stress development for an aerospace grade material system. The characterized interfacial stresses are then validated by fabricating long and symmetric laminates using similar pressures as DMA tests and measuring process-induced warpages. The results of this study are intended to expand the current understanding of tool-part interaction, provide a framework for more robust simulation capabilities, and potentially mitigate PIDs in composites processing.

CHARACTERIZING TOOL-PART INTERACTION

Materials

The composite material used in this study was Toray T800S/3900-2 UD prepreg with a resin content of 35% by weight [15]. 3900-2 is a toughened aerospace grade epoxy resin, while T800S is a carbon fiber with intermediate modulus and high strength. In addition to epoxy resin, the prepreg's interlayer regions and surface contain micro-spherical thermoplastic tougheners with a glass transition temperature (T_g) of about 150 °C [16,17]. In recent decades, the T800/3900-2 system has been used as a primary structural material on major aircraft such as the Boeing 787.

The release coating used in this study was Loctite® Frekote® 710-NC™ release agent. The exact formulations of Frekote products are proprietary, but basic information of 710-NC is provided in publicly available datasheet [18]. The composition by weight of Frekote 710-NC release agent includes 1-5% silicone components (reaction product of TMAS and PDMS), 1-5% octane, 1-5% hydrocarbons (C7-10), 60-100% petroleum as the carrier, and 10-30% dibutyl ether as the solvent. Polydimethylsiloxane (PDMS) acts as the active silicone in 710-NC release agent, which gives the product its high abhesion (i.e., low surface free energy) and high chemical/thermal stability properties [19]. After the release agent (RA) is applied on a tool, most of the carrier and solvent evaporate, while the silicones and hydrocarbons remain on the tool surface.

Sample Preparation

Sample preparation consisted of creating and debulking two cross-ply composite laminates. First, ten plies of T800S/3900-2 with nominal dimensions of 4 mm × 4 mm were cut using an X-ACTO® knife. The plies were then stacked to create two cross-ply laminates, each with a $[90/0/\overline{90}]_s$ layup. Next, both laminates were simultaneously hot-debulked for 30 minutes at 60 °C on a hotplate under approximately 0.7 MPa of applied pressure from caul plates. The laminates were then removed from the hot plate and cooled down to room temperature before testing in the DMA.

Apparatus

Fig. 2 shows an image of the custom fixture built to directly measure interfacial shear stresses. The setup was constructed using the shear sandwich clamp in a TA Instruments® Discovery Dynamic Mechanical Analyzer (DMA) 850, and custom-machined U- and C-shape components to cover the moveable and stationary clamps. All custom tools were made from A2 tool steel and machined to fit securely in the test fixture. The U-shape tool was reused throughout the entire testing campaign, while two new C-shape tools were prepared for each test using a manual shear/brake combination machine.

Before each test, the U-shape tool was cleaned with Loctite® Frekote® PMC™ mold cleaner to remove any surface residue from previous testing or handling. Then, each outside surface on the U-shape tool was treated with three layers of Frekote 710-NC release agent using a brush, allowing 15 minutes between coats as recommended on the product's datasheet [18]. The outside surfaces of the C-shapes were roughened using 80 grit aluminum oxide sandpaper for two minutes. The abraded surfaces were then cleaned with isopropyl alcohol (IPA) to remove any steel dust created during sanding. After all custom tools were prepared and secured over the DMA clamps, the composite laminates were sandwiched between the U- and C-shapes with the 90° plies facing horizontally. Compaction pressure was applied to the laminates using the knurled knobs and monitored throughout the cure cycle by placing FlexiForce™ HT201 piezoresistive force sensors between each stationary clamp and C-shape tool [20].

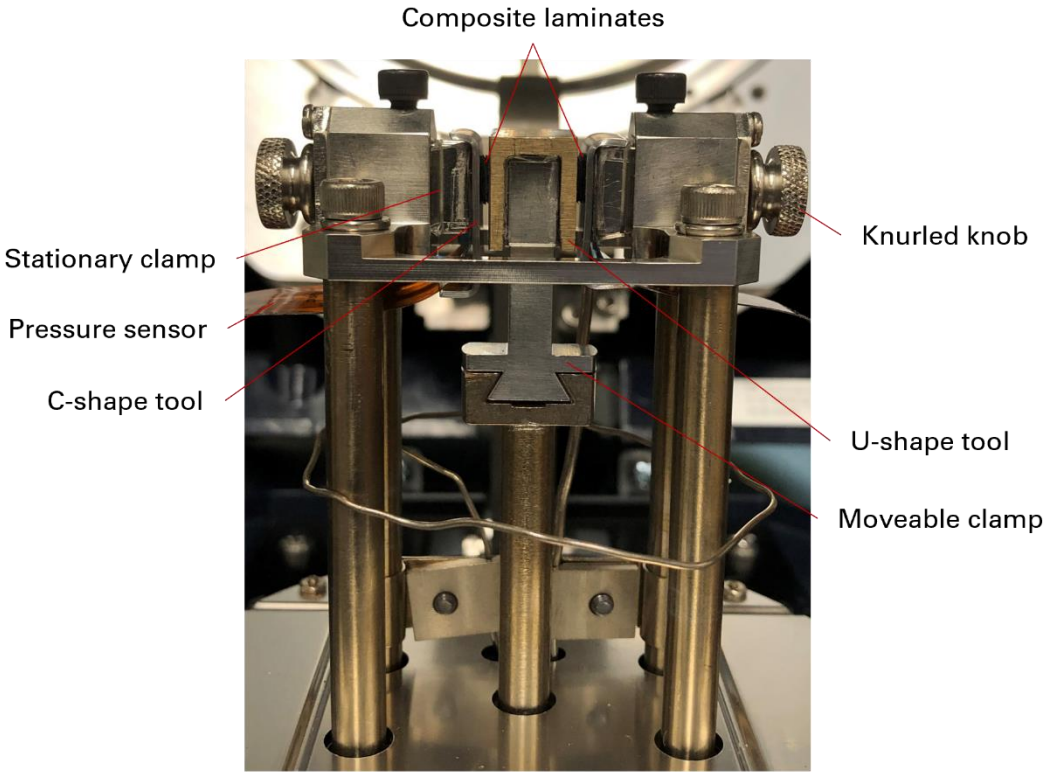

Figure 2. Custom DMA shear test set-up used for measuring tool-part interfacial stress developments during processing cycles.

Test Procedure

Once the composite samples were loaded into the DMA shear sandwich fixture, the system was subjected to a temperature cycle following the Manufacturer's Recommended Cure Cycle (MRCC) [15]. The temperature cycle consisted of heating to 180 °C at 2 °C/min, holding at 180 °C for 120 minutes, then cooling the system down. Five different pressures of 101, 222, 347, 555, and 763 kPa were applied to the composite laminates throughout the testing campaign. Two tests were conducted at each pressure for a total of ten tests. During the heat-up stage of the cure cycle, the laminates begin to cure, and the outwards-facing plies form strong primary bonds and mechanical bonds with the abraded C-shape tool surfaces. The composites thus remain bonded and fixed to the stationary C-shapes throughout the test. The inwards-facing plies of the laminates form weaker primary and secondary bonds with the U-shape tool since its surfaces are covered with RA. The laminates are held stationary during cure until their gel points, where tool-part stresses start to evolve [8,9]. Gelation was estimated to occur 90 minutes into the cure cycle based on previous studies [2].

Upon gelation, an upwards force was applied from the DMA drive motor to generate vertical motion in the U-shape tool. This created a constant strain rate which was applied through the remaining time of the 180 °C temperature hold. Due to equipment limitations of the DMA, the strain rate could not be applied during cool-down, and thus the cooling stage of the cure cycle was neglected in this study. As previously mentioned, the composite samples remained stationary throughout the cure cycle as they were

strongly bonded to the outside C-shapes. The relative movement between the U-shape tool and composites simulated a tool-part shear interaction during processing due to mismatches in free strains. A displacement rate of 0.05 mm/min was chosen for all tests based on a previous study by Ersoy et al. [9]. The DMA automatically measured and recorded forces needed to produce the tool-part shear strain throughout the cure cycle. The recorded forces were then divided by the effective sample area to calculate tool-part interfacial shear stresses.

TOOL-PART INTERACTION TEST RESULTS AND DISCUSSION

Fig. 3 shows the development of tool-part interfacial stresses ($\tau_{tool\text{-}part}$) throughout the MRCC while applying a pressure of 763 kPa. The temperature profile (T), simulated glass transition temperatures of resin and thermoplastic particles (T_g^R and T_g^P, respectively), and degree of cure (DoC) are also shown in the graph. Tool-part stresses were confined at zero until the strain rate was applied at the gel point 90 minutes into the cure cycle. Upon gelation, tool-part stresses evolved linearly, reached a maximum value, sharply dropped, then decreased non-linearly through the remainder of the isothermal hold at 180 °C.

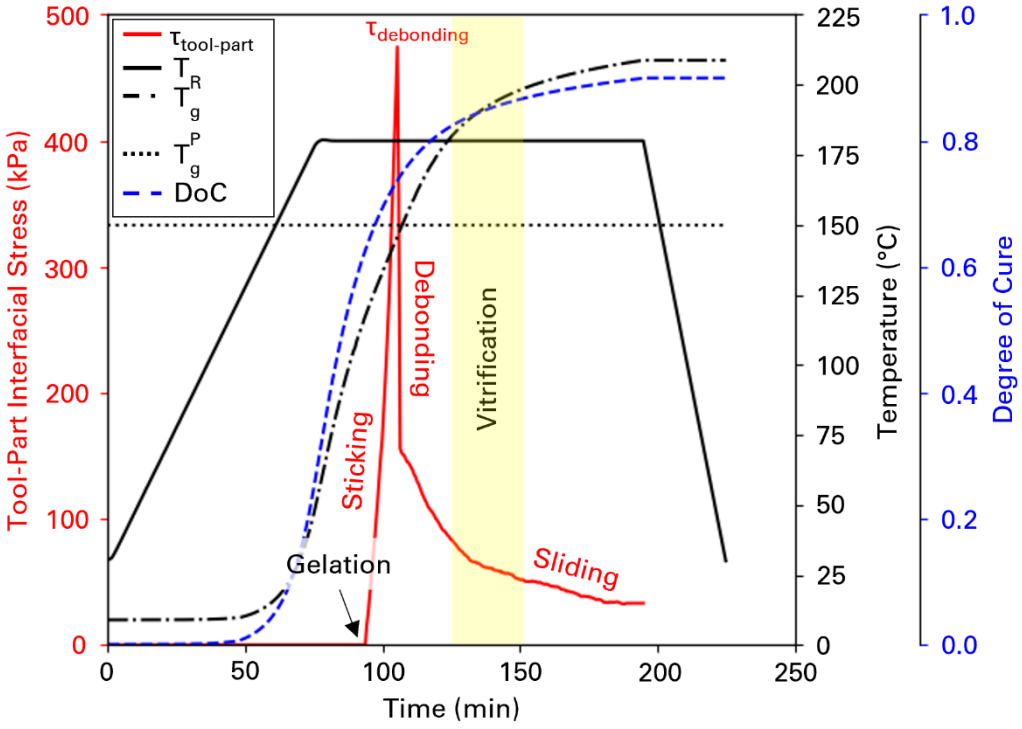

Figure 3. Tool-part interfacial stress development between T800S/3900-2 laminates with $[90/0/\overline{90}]_s$ lay-ups and a steel tool covered with three layers of Frekote 710-NC release agent. 763 kPa of compaction pressure was applied throughout processing.

The initial rise in stress upon gelation represents sticking or static friction between the tool and part [8,9,11]. At this stage of the cure cycle, the resin has transformed from a viscous fluid to a rubbery solid. Since the processing temperature at gelation is well above the glass transition temperature of the thermoplastic particles, these components are similarly in a rubbery state [16]. The friction between a rubbery solid and hard surface (e.g., a tool) is mainly controlled by two mechanisms: interfacial adhesion and internal viscoelastic deformations. Resistive mechanical forces also contribute to friction between any two solid bodies but may be considered negligible when one of the solids is a soft rubber [21]. Interfacial adhesion directly results from surface free energy effects causing the polymer chains in the rubber to form adhesive bonds and become "pinned" to the hard surface. On the other hand, internal viscoelastic contributions arise due to friction between polymer chains in the bulk of the rubber. When subjected to normal pressure and in-plane strain, oscillating forces are exerted on the rubber, leading to energy dissipation via internal viscoelastic friction between the rubber's polymer chains [21]. Since Frekote 710-NC release agent with exceptionally low surface free energy properties (i.e., 10-20 mJ/m^2) was applied to the tool prior to processing, it is unlikely that strong interfacial adhesive bonds formed during the cure cycle [19]. Therefore, the linear increase in stress upon gelation was primarily due to internal strain-resistive viscoelastic friction in the composite's resin and thermoplastic particles, given that both components were in the rubbery regime. Mechanical friction between the tool and any exposed fiber surfaces may also potentially contribute to this stress.

After approximately ten minutes (i.e., 0.5 mm) of applied strain, interfacial stresses reached a maximum value of 477 kPa before sharply dropping. This maximum value of stress is often referred to as the tool-part debonding stress ($\tau_{debonding}$) and signifies the transition from static to kinetic friction. Debonding occurred while the resin and thermoplastic particles were still in their rubbery states. A broken tool-part bond at this stage of the cure cycle may thus be described as the polymer chains on the composite part's surface undergoing a rapid "snapping" or "unpinning" from the tool [21]. The measured debonding stress was approximately 30 kPa higher than previous results in the literature for a non-toughened AS4/8552 material system under a similar but slightly lower cure pressure [9]. These results suggest that thermoplastic toughening particles may affect tool-part bonding during a cure cycle.

The post debonding regime in Fig. 3 shows a sharp drop in stress to an intermediate value of approximately 150 kPa, then a non-linear decline through the remainder of the isothermal hold. The gradual stress decay represents sliding or kinetic friction between the tool and part [8,9,11]. Immediately after tool-part debonding occurred, the glass transition temperature of the resin was rapidly evolving and approaching the processing temperature. However, the thermoplastic particles' glass transition temperature remained constant and below 180 °C until the end of the cure cycle. In other words, the composite's resin was transitioning from a rubbery viscoelastic body to a glassy elastic solid, while the thermoplastic particles remained in a rubbery state. The resin's transition to an elastic solid would consequently be accompanied by a reduction of the viscoelastic friction contributions and thus a direct decline in overall sliding stress values, shown in Fig. 3.

Upon reaching the vitrification zone, the resin begins acting like an elastic solid and the dominant strain-resistive contribution shifts to mechanical friction with the tool [11,22]. Mechanical friction may be thought of as material asperities at the tool-part interface resisting elastic deformation during the applied strain. At the end of the

isothermal hold, the resin is a fully elastic solid and its viscoelastic contributions to friction are minimal. The final sliding stress value of approximately 30 kPa was thus primarily determined by mechanical friction in the resin and internal viscoelastic effects in the thermoplastic particles.

Fig. 4 shows tool-part interfacial stress versus strain throughout the MRCC for five cure pressures ranging from 101 to 763 kPa. The profiles shown in red represent the first DMA test conducted at each pressure, while purple curves correspond to duplicate tests. In all ten tests, the applied strain at gelation caused sharp linear increases in stress. These results indicate that a tool and composite part exhibit sticking behavior regardless of cure pressure. All stress profiles then progressed to maximum values where debonding occurred ($\tau_{debonding}$). The magnitudes of debonding stresses demonstrated a non-linear relationship with cure pressure, with the lowest and highest values occurring at 101 and 347 kPa, respectively. These results differ from Amontons' first law, which states that friction (e.g., debonding stress) between two hard bodies is mechanically-driven and directly proportional to the normal force (e.g., pressure) pushing the objects together [22]. The non-linearity in debonding stresses demonstrates that Amontons' law breaks down when one of the bodies is in a rubbery state, such as the T800S/3900-2 laminate between gelation and vitrification. Furthermore, the results suggest that debonding stresses were not purely mechanically-driven, but instead highly influenced by bulk viscoelastic effects in the composite part.

After debonding, all stress profiles showed non-linearly decaying sliding regimes in response to vitrification and the transition to mechanical friction forces. At the end of the isothermal hold, the highest sliding stresses were measured at 555 kPa, while the lowest occurred at 100 kPa. Overall, Fig. 4 demonstrates that the applied pressure significantly affects tool-part stress developments throughout a cure cycle.

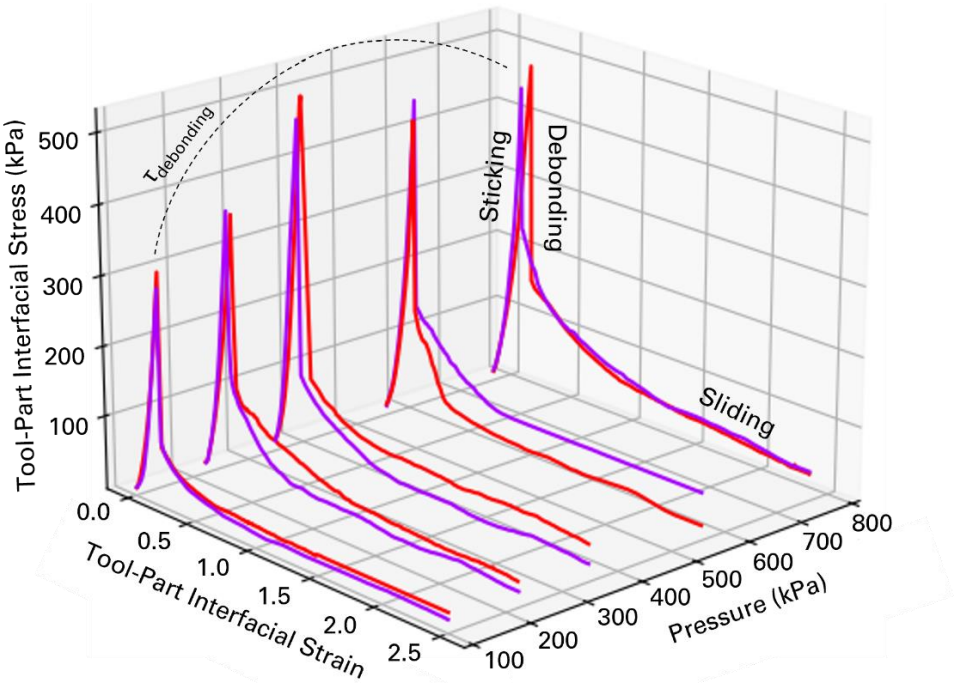

Figure 4. Tool-part interfacial stress developments measured in the custom DMA fixture for five different applied pressures.

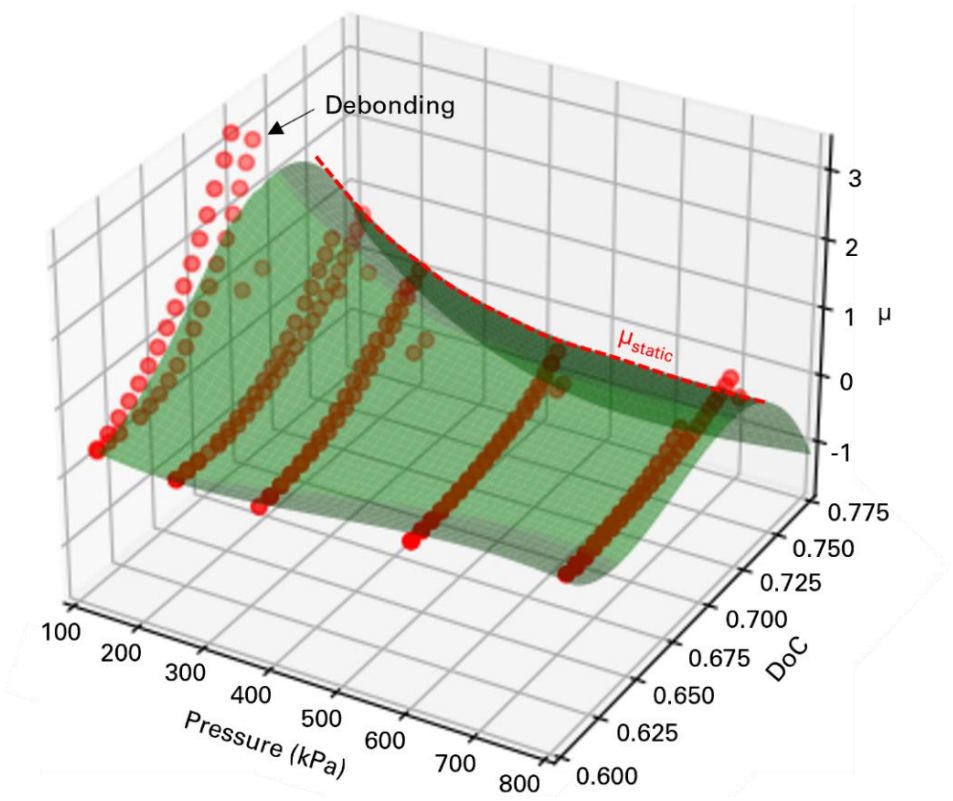

Figure 5. Friction coefficients (μ) in the tool-part sticking regime as functions of applied pressure and degree of cure (DoC).

Fig. 5 breaks down the sticking (i.e., static friction) regimes of the stress profiles reported in Fig. 4. The plot shows coefficient of friction values as functions of pressure and degree of cure. Friction coefficients were calculated by dividing tool-part stresses by their respective applied pressures. Each coefficient value in Fig. 5 may be thought of as normalized friction with respect to pressure. A response surface, shown in green, was fitted to the data using a supervised machine learning (ML) method, Gaussian Process Regression (GPR) with an accuracy of 79%. The plot only shows values up to the debonding point of each test, where the tool-part interaction transitions to kinetic friction. Tool-part debonding occurred within a narrow window of 70-74% degree of cure in all DMA tests. The friction coefficient when debonding occurs is considered the static friction coefficient (μ_{static}).

The plot in Fig. 5 demonstrates that pressure has non-linear inverse effects on static friction coefficients between a tool and a T800S/3900-2 composite part. Previous results in the literature have shown similar trends between composite prepreg and a tool surface [11]. However, the reported tests were conducted with a different material system in its pre-gelation stage (i.e., DoC = 20%). The reduction in static friction was attributed to a pressure-induced decrease in the part's surface roughness and consequent decline in mechanical resistance to the moving tool. However, as previously discussed, tool-part bonding and thus static friction in the DMA tests were not mechanically-driven. Therefore, reduced composite surface roughness was not likely the principal contributor to the drop in static friction coefficient with pressure. Instead, the trends observed in Fig. 5 were likely due to changes in viscoelastic effects in the composites. Applying

higher pressure to composite laminates during processing, leads to an increase in thermoplastic particle aspect ratio and volume fraction in the interlayer region adjacent to the tool surface, and hence a reduction in the resin fraction [16,17]. These effects may reduce the tool-part static friction coefficient, as demonstrated in Fig. 5.

Fig. 6 focuses on the sliding (i.e., kinetic friction) regimes of the stress profiles reported in Fig. 4. The plot shows kinetic friction coefficient values as functions of pressure and differences between processing temperature and the resin's instantaneous glass transition temperature ($T - T_g^R$). The friction coefficient at each point after debonding occurs is considered the kinetic friction coefficient ($\mu_{kinetic}$). A response surface, shown in green, was fitted to the data using GPR with an accuracy of 89%. The plot in Fig. 6 reveals that pressure also has inverse effects on kinetic friction coefficients. These effects are more distinct prior to vitrification, but are still evident after the resin becomes a glassy solid. This can also be attibutued to an increase in the thermoplastic fraction at the interface at higher pressures. These effects would cause tool-part kinetic friction coefficients at higher pressures to be less dependent on the evolution of the resin's glass transition temperature. This is further supported by the most gradual decrease in $\mu_{kinetic}$ with the evolution of T_g^R at the highest processing temperature of 763 kPa.

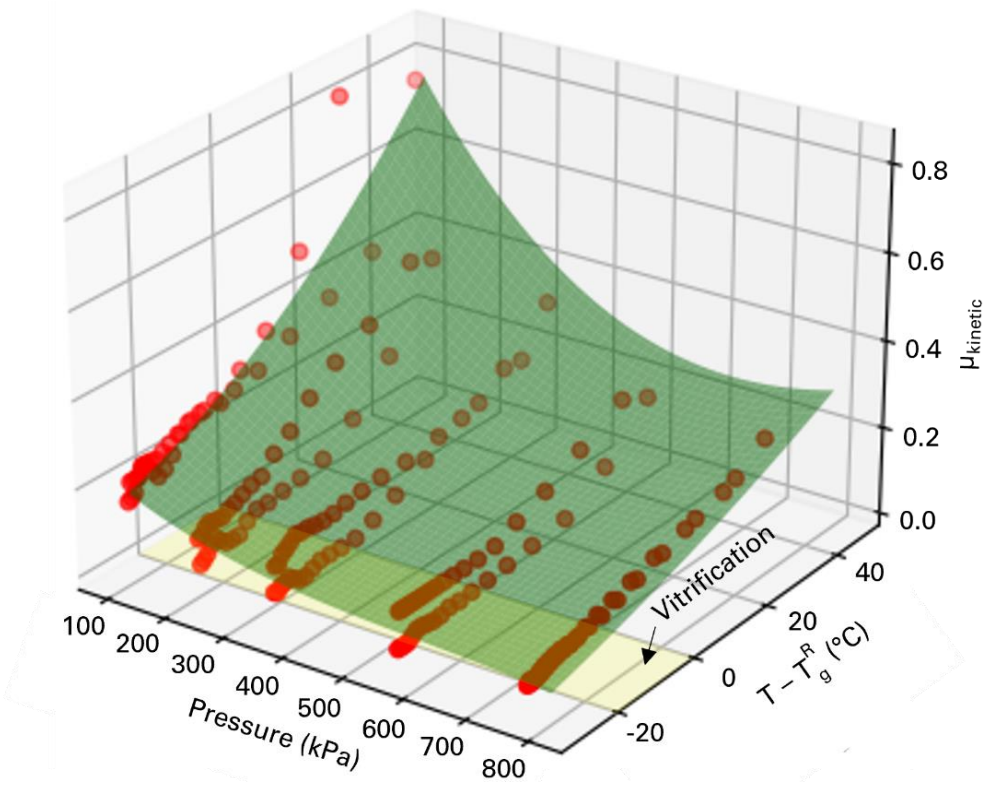

Figure 6. Kinetic friction coefficients ($\mu_{kinetic}$) in the tool-part sliding regime as functions of applied pressure and difference between processing temperature and instantaneous resin glass transition temperature of T800S/3900-2 prepreg ($T - T_g^R$).

VALIDATION TESTS

Validation tests consisted of curing long and symmetric composite parts in an autoclave under different pressures and measuring the final warpages after demolding. A typical prepreg lay-up and vacuum bagging procedure was used to fabricate the composite parts. First, a flat mirror-like plate made of A2 tool steel was treated with three layers of 710-NC release agent using a brush. The tool surface was cleaned with PMC mold cleaner and retreated with three layers of 710-NC before each test. Then, two 90-degree plies of T800S/3900-2 prepreg with nominal dimensions of 80 mm (w) × 400 mm (l) were cut using an X-ACTO® knife. The plies were then stacked on the tool surface to create a $[90]_2$ laminate. Next, the tool and composite laminate were covered with one sheet of fluorinated ethylene propylene (FEP) release film. A caul plate was then placed on top of the FEP directly over the laminate to ensure volume fraction symmetry in the part. FEP between the caul plate and laminate acted as a barrier to restrict any interfacial adhesive bonding between the top surface of the part and the caul plate. The tool and lay-up were then covered by one layer of breather cloth, sealed in vacuum bagging, loaded into an autoclave, and subjected to the MRCC under different pressures. Five different cure pressures were used for validation tests: 101, 239, 412, 584, and 715 kPa. After a cure cycle was completed, the composite part was demolded and the maximum warpage was measured using a Keyence LJ-X8400 2D laser profiler.

WARPAGE TEST RESULTS AND DISCUSSION

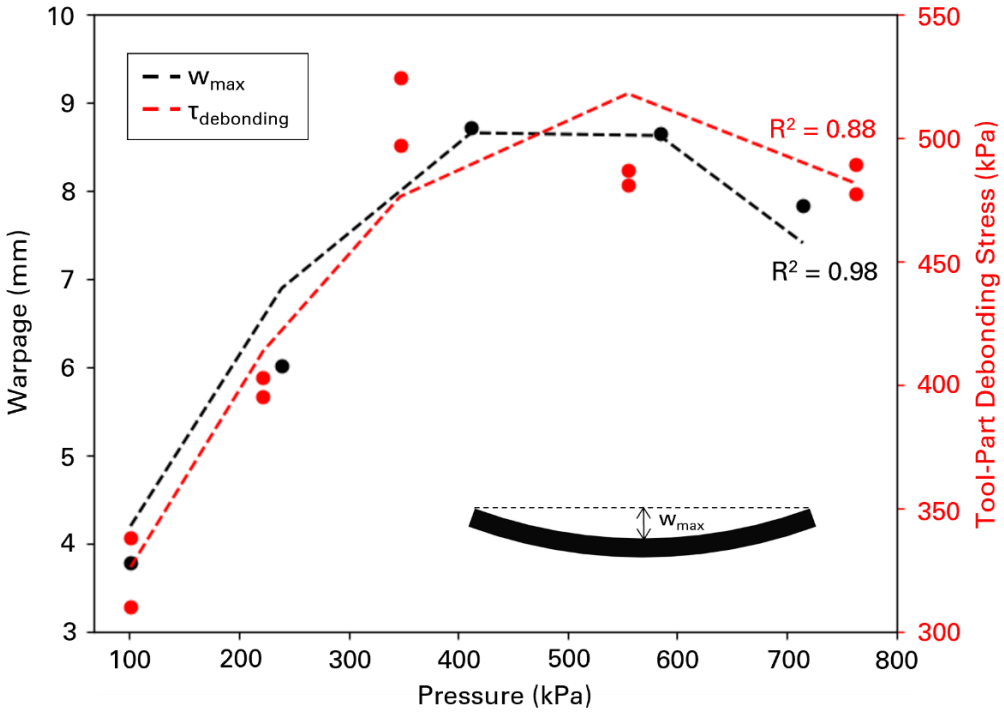

Figure 7. Maximum warpage (w_{max}) of $[90]_2$ composite parts cured in an autoclave and tool-part debonding stresses measured during DMA testing for five cure pressures.

Fig. 7 shows warpage magnitudes of the $[90]_2$ laminates cured under five different pressures. Experimental measurements are shown as black points in the plot. A trendline was fitted to the data for illustration purposes only. Warpage values ranged from approximately 3 to 9 mm, with the highest value occurring at an intermediate pressure value of 412 kPa. These results show a relationship between warpage and pressure similar to the trends for debonding stresses measured in the DMA (also shown in Fig. 7). This suggests that maximum warpage values may be inferred or predicted from the tool-part debonding stress. Although the non-linear warpage relationship validates the existence of multi-physics interactions at the tool-part interface, additional work must be conducted to fully understand the complexities of the underlying problem. Some future work includes analyzing the effects of cure pressure on the ply thickness and surface morphology of the composite parts.

CONCLUSIONS

The main objective of this study was to investigate the effects of cure pressure on tool-part interaction for Toray T800S/3900-2. A custom DMA shear test setup was built to achieve this goal. The novel technique was utilized to characterize the development of tool-part interfacial stresses and friction throughout a cure cycle for five different applied pressures. The warpage values of flat laminates cured under similar conditions were used to validate the DMA results. The main conclusions from this work are as follows:

- Tool-part interfacial stresses and friction for T800S/3900-2 are non-linearly affected by cure pressure. The highest tool-part debonding stresses occur between intermediate pressures of approximately 300-500 kPa. The highest tool-part static and kinetic friction occur at low pressures of around 100 kPa. The non-linear relationships between tool-part debonding, friction, and pressure are likely due to multi-physics viscoelastic interactions occurring in the bulk of the composite part and at the tool-part interface.
- The warpage of flat $[90]_2$ T800S/3900-2 parts may be directly related to the tool-part debonding stress. Maximum warpage shows similar trends as debonding stress with pressure, with the highest values occurring at the intermediate pressure range of approximately 300-500 kPa.

ACKNOWLEDGEMENTS

The work reported here was funded by Toray Industries, Inc.

REFERENCES

1. Zobeiry N. and A. Poursartip. 2015. “The origins of residual stress and its evaluation in composite materials,” in Structural Integrity and Durability of Advanced Composites, P.W.R. Beaumont, S. Soutis, and A. Hodzic, eds. Woodhead Publishing, pp. 43-72.
2. Zobeiry, N., A. Forghani, C. Li, K. Gordnian, R. Thorpe, R. Vaziri, G. Fernlund, A. Poursartip. 2016. “Multiscale characterization and representation of composite materials during processing,” Phil. Trans. R. Soc. A, 374: 20150278.

3. Fernlund G., C. Mobuchon, and N. Zobeiry. 2018. “2.3 Autoclave Processing,” in Comprehensive Composite Materials II, P.W.R. Beaumont and C.H. Zweben, eds. Oxford: Academic Press, pp. 42-62.
4. Li, C., N. Zobeiry, S. Chatterjee, and A. Poursartip. 2014. “Advances in the characterization of residual stress in composite structures,” in SAMPE Conf., Society for the Advancement of Material and Process Engineering, Seattle, WA.
5. Twigg, G., A. Poursartip, and G. Fernlund. 2004. “Tool–part interaction in composites processing. Part I: experimental investigation and analytical model,” Composites Part A: Applied Science and Manufacturing, 35(1): 121-133.
6. Twigg, G., A. Poursartip, and G. Fernlund. 2004. “Tool–part interaction in composites processing. Part II: numerical modelling,” Composites Part A: Applied Science and Manufacturing, 35(1): 135-141.
7. Potter, K. D., M. Campbell, C. Langer, and M. R. Wisnom. 2005. “The generation of geometrical deformations due to tool/part interaction in the manufacture of composite components,” Composites Part A: Applied Science and Manufacturing, 36(2): 301-308.
8. Twigg, G., A. Poursartip, and G. Fernlund. 2003. “An experimental method for quantifying tool– part shear interaction during composites processing,” Composites Science and Technology, 63(13): 1985-2002.
9. Ersoy, N., K. Potter, M. R. Wisnom, and M. J. Clegg. 2005. “An experimental method to study the frictional processes during composites manufacturing,” Composites Part A: Applied Science and Manufacturing, 36(11): 1536-1544.
10. Zappino, E., N. Zobeiry, M. Petrolo, R. Vaziri, E. Carrera, and A. Poursartip. 2020. “Analysis of process-induced deformations and residual stresses in curved composite parts considering transverse shear stress and thickness stretching,” Composite Structures, 241: 112057.
11. Kaushik, V. and J. Raghavan. 2010. “Experimental study of tool–part interaction during autoclave processing of thermoset polymer composite structures,” Composites Part A: Applied Science and Manufacturing, 41(9): 1210–1218.
12. Albert, C. and G. Fernlund. 2002. “Spring-in and warpage of angled composite laminates,” Composites Science and Technology, 62(14): 1895–1912.
13. Takagaki, K., Minakuchi, S., and Takeda, N. 2017. “Process-induced strain and distortion in curved composites. Part I: Development of fiber-optic strain monitoring technique and analytical methods,” Composites Part A: Applied Science and Manufacturing, 103: 236–251.
14. Fernlund, G., Abdel-Rahman, N., Courdji, R., Poursartip, A., Willden, K., Nelson., K. 2002. “Experimental and numerical study of the effect of cure cycle, tool surface, geometry, and lay-up on the dimensional fidelity of autoclave-processed composite parts,” Composites Part A: Applied Science and Manufacturing, 33(3): 341–351.
15. Toray Composite Materials America, Inc. 2020. “3900 PREPREG SYSTEM”.
16. Chen, C., Poursartip, A., and Fernlund, G. 2020. “Cure-dependent microstructures and their effect on elastic properties of interlayer toughened thermoset composites,” Composites Science and Technology, 197: 108241.
17. Chen, C., Poursartip, A., and Fernlund, G. 2021. “Influence of the glass transition of interlaminar particles on shear behaviour during cure of interlayer toughened thermoset composites,” Composites Part A: Applied Science and Manufacturing, 147: 106447.
18. Henkel Corporation, “TDS Loctite® Frekote® 710-NC™,” 2015.
19. Critchlow, G.W., Litchfield, R. E., Sutherland, I., Grandy, D.B., and Wilson, S. 2006. “A Review and Comparative Study of Release Coatings for Optimised Abhesion in Resin Transfer Moulding Applications.” International Journal of Adhesion and Adhesives, 26(8): 577-599.
20. Tekscan, Inc., “FlexiForce™ Standard Model HT201,” 2021.
21. Persson, B.N.J. 1998. “On the theory of rubber friction,” Surface Science, 401(3): 445–454.
22. Otsuki, M., and Matsukawa, H. 2013. “Systematic Breakdown of Amontons’ Law of Friction for an Elastic Object Locally Obeying Amontons’ Law,” Scientific Reports, 3(1): 1586.